

Osteoarthritis and Cartilage (2009) 17, 953–960

© 2008 Osteoarthritis Research Society International. Published by Elsevier Ltd. All rights reserved.

doi:10.1016/j.joca.2008.12.002

Osteoarthritis and Cartilage



International
Cartilage
Repair
Society



Solidification mechanisms of chitosan–glycerol phosphate/blood implant for articular cartilage repair

C. Marchand[†], G.-E. Rivard[‡], J. Sun[§] and C. D. Hoemann^{†||*}

[†] *Institute of Biomedical Engineering, Ecole Polytechnique, Montreal, QC, Canada*

[‡] *Division of Hematology–Oncology, Hôpital Sainte-Justine, Montreal, QC, Canada*

[§] *Bio Syntech Canada Inc., Laval, QC, Canada*

^{||} *Department of Chemical Engineering, Ecole Polytechnique, Montreal, QC, Canada*

Summary

Objective: Chitosan–glycerol phosphate (chitosan-GP) is a unique polymer solution that is mixed with whole blood and solidified over microfractured or drilled articular cartilage defects in order to elicit a more hyaline repair cartilage. For clinical ease-of-use, a faster *in situ* solidification is preferred. Therefore, we investigated the mechanisms underlying chitosan–GP/blood implant solidification.

Methods: *In vitro* solidification of chitosan–GP/blood mixtures, with or without added clotting factors, was evaluated by thromboelastography. Serum was analyzed for the onset of thrombin, platelet, and FXIII activation. *In vivo* solidification of chitosan–GP/blood mixtures, with and without clotting factors, was evaluated in microdrilled cartilage defects of adult rabbits ($N = 41$ defects).

Results: Chitosan–GP/blood clots solidified in an atypical biphasic manner, with higher initial viscosity and minor platelet activation followed by the development of clot tensile strength concomitant with thrombin generation, burst platelet and FXIII activation. Whole blood and chitosan–GP/blood clots developed a similar final clot tensile strength, while polymer–blood clots showed a unique, sustained platelet factor release and greater resistance to lysis by tissue plasminogen activator. Thrombin, tissue factor (TF), and recombinant human activated factor VII (rhFVIIa) accelerated chitosan–GP/blood solidification *in vitro* ($P < 0.05$). Pre-application of thrombin or rhFVIIa + TF to the surface of drilled cartilage defects accelerated implant solidification *in vivo* ($P < 0.05$).

Conclusions: Chitosan–GP/blood implants solidify through coagulation mechanisms involving thrombin generation, platelet activation and fibrin polymerization, leading to a dual fibrin–polysaccharide clot scaffold that resists lysis and is physically more stable than normal blood clots. Clotting factors have the potential to enhance the practical use, the residency, and therapeutic activity of polymer–blood implants.

© 2008 Osteoarthritis Research Society International. Published by Elsevier Ltd. All rights reserved.

Key words: Chitosan, Articular cartilage repair, Microfracture, Coagulation, Blood, Platelets, Platelet factor 4, Factor XIII, Factor VIIa, Thrombin, Tissue factor, Thrombin–antithrombin (TAT).

Introduction

A current aim and major challenge in orthopedic practice is to regenerate durable cartilage in focal articular lesions^{1–3}. Cartilage is avascular and when damaged fails to bleed and therefore lacks an efficient wound repair response. To stimulate a natural wound response, surgeons have developed techniques like bone marrow stimulation involving drilling or microfracture in the base of the débrided cartilage lesion to induce subchondral bleeding and generate conduits to permit bone marrow stem cell migration into the cartilage lesion^{3–6}. However in skeletally mature human patients and animal models, these surgical techniques principally result in the formation of a repair tissue predominantly composed of fibrous tissue or fibrocartilage, tissue types with weak biomechanical properties compared to hyaline articular cartilage^{2,5,7–13}. Treatments that improve the volume,

integration, and hyaline quality of marrow-derived repair tissue are therefore the focus of intense research.

Bleeding and the formation of a blood clot are initiating events of microfracture therapy⁶, however the clot is best retained in the bone defect and not on the cartilage surface^{14–16}. To improve clot retention in the cartilage lesion following microfracture and drilling, we previously developed a scaffold-stabilized blood clot using chitosan, a cationic, adhesive and biocompatible polysaccharide. Homogenous mixtures of autologous whole blood and solutions of chitosan–glycerol phosphate (chitosan–GP) solidify to form a clot with morphologically normal erythrocytes and a structurally stable fibrous network with chitosan and fibrin fibers^{17,18}. Hybrid chitosan clots resist platelet-mediated clot retraction, and remain voluminous, firm and elastic¹⁷. The formation of a chitosan–GP/blood clot in marrow-stimulated cartilage defects in sheep and rabbit improved the quantity, hyaline quality and integration of repair cartilage with porous subchondral bone compared to repair tissue formed by microfracture or drilling alone^{17,19}. Hybrid clots were shown to promote hyaline repair by attracting neutrophils, marrow-derived repair cells, and by stimulating transient angiogenesis and bone remodeling¹⁵.

*Address correspondence and reprint requests to: Caroline D. Hoemann, Department of Chemical Engineering, Ecole Polytechnique Montreal, 2900 Boul. Edouard Montpetit, Montreal, QC H3C 3A7, Canada. Tel: 1-514-340-4848; Fax: 1-514-340-2980; E-mail: caroline.hoemann@polymtl.ca

Received 17 April 2008; revision accepted 6 December 2008.

Mixture of liquid chitosan–GP into whole blood generates a hybrid clot implant that forms within 10–15 min after depositing in large animal or patient microfracture defects^{19,20}. A more rapid implant solidification could facilitate treatment of larger defects with curved surfaces and unconfined borders, and also reduce the length of the cartilage repair procedure. Indeed, for clinician ease-of-use, a faster and controlled *in situ* solidification is preferred; however solidification mechanisms are incompletely understood. Many studies previously demonstrated that acidic chitosan solutions and solid chitosan particles are thrombogenic, through mechanisms involving red blood cell (RBC) agglutination, and platelet activation, without direct activation of the clotting cascade^{17,21–23}. By comparison, little is understood concerning the hemostatic properties of isotonic and near-neutral pH chitosan–GP solutions.

The first aim of the current study was to elucidate solidification mechanisms of chitosan–GP/blood *in vitro*, using a Thromboelastograph® (TEG), an instrument that measures clotting time and clot tensile strength. We tested the hypothesis that chitosan–GP/blood solidification is thrombin-dependent, and furthermore implicates platelet and Factor XIII activation. The second aim of this study was to develop novel methods to accelerate *in situ* solidification in an *in vivo* animal cartilage repair model. We therefore tested the hypothesis that *in vivo* solidification of chitosan–GP/blood mixtures in microdrilled articular cartilage defects can be accelerated using clotting factors including thrombin (IIa), tissue factor (TF) and recombinant human factor VIIa (rhFVIIa). Tissue factor is a transmembrane receptor constitutively expressed in mainly extravascular tissues. TF binding with trace amounts of activated FVIIa that are present in plasma²⁴ triggers the extrinsic clotting cascade and thrombin generation. In our *in vivo* experiments, we used a recombinant TF–phospholipid preparation at concentrations previously employed in clinical applications for maxillary bone grafts²⁵, rhFVIIa at concentrations around threefold greater than the target plasma levels for clinical applications (~2 µg/mL)²⁶, and thrombin concentrations within the low range used in standard fibrin glue²⁷. Our choice of these particular factors was thus based on their known ability to promote repair processes, as well as their current use in other clinical contexts which could help translate their use in cartilage repair strategies involving polymer–blood implants.

Materials and methods

MATERIALS

Medical-grade sterile solutions of chitosan (2.05% w/v, 80% degree of deacetylation, DDA, 1200–2000 mPa s., pH 5.6, <100 EU/mL endotoxins units and <5 ppm heavy metal content) and 500 mM disodium β-glycerol phosphate/50 mM HCl pH 7.1 (GP) were provided by Bio Syntech Inc (Laval, QC, Canada). Chitosan–GP solutions were formed aseptically by combining 1.2 mL chitosan–HCl with 0.3 mL GP. Rhodamine B-isothiocyanate (RITC)–chitosan 0.5% mol/mol RITC/chitosan (80.5% DDA, M_n 144 kDa, polydispersity (M_w/M_n) 1.3) was prepared as 5 mg/mL filter-sterile solutions as previously described²⁸. Calibrated viscosity standards (N62000, N1000, S60) were from Canon Instrument Company (State College, PA, USA) and silicon oil (pure silicone fluid) was from Clearco Products (Bensalem, PA, USA). Other reagents included sterile recombinant human Factor VIIa (NovoNordisk, Copenhagen, Denmark), tissue culture-grade purified human thrombin and benzamidine (Sigma–Aldrich, Oakville, ON, Canada), TF (Innovin®) and thrombin–antithrombin (TAT) enzyme-linked immunosorbent assay (ELISA) kits (Dade Behring, Mississauga, ON, Canada), and pooled normal plasma for TAT ELISA sample dilution (Precision Biologic, Dartmouth, Nova Scotia, Canada), affinity-purified goat anti-human platelet factor 4 (PF4) antibody (R&D Systems, Cedarlane, Burlington, ON, Canada), sheep anti-human A and B subunit of Factor XIII (FXIII) antibody and Phe-Pro-Arg-chloromethylketone, a thrombin protease

inhibitor (FPR-ck), purified human PF4 and human FXIII (Haematologic Technologies, Essex Junction, VT, USA), donkey anti-goat-horseradish peroxidase (HRP) and donkey anti-sheep-HRP (Jackson Immunology, Montreal, QC, Canada), chemiluminescence substrate kit (Lumi-light, Roche Diagnostics, QC, Canada), and Hyperfilm ECL (Amersham Biosciences, GE Health, ON, Canada). Recombinant tissue plasminogen activator [tPA 1 mg/mL, diluted to 2 µg/mL in phosphate-buffered saline (PBS) with 4% w/v bovine serum albumin (BSA)] was from Hoffmann-La Roche (NJ, USA). Ringer's lactated saline (RLS) buffer (Baxter) was purchased from Lavigne & Dufort (Montreal, QC, Canada).

CLOTTING FACTOR PREPARATION FOR *IN VITRO* AND *IN VIVO* EXPERIMENTS

Factor rhFVIIa was reconstituted with sterile water for injection from Abbott (QC, Canada) at 500 µg/mL. Purified human IIa lyophilized powder containing 0.15 M sodium chloride and 0.05 M sodium citrate buffer at pH 6.5 was reconstituted with sterile water for injection at 100 U/mL. Innovin® or recombinant TF containing phospholipids was freshly reconstituted with 2 mL sterile water for injection, to give 5 nM TF according to a recombinant TF standard curve (S. Butenas, personal communication)²⁹. For *in vitro* TEG experiments, clotting factors were diluted with RLS before loading in the TEG cups.

COAGULATION ANALYSES BY THROMBOELASTOGRAPHY, ELISA AND WESTERN BLOT

Clot tensile strength was evaluated for up to 180 min with four Thromboelastograph® (TEG) (5000 series TEG analyzer Software Version 3, Haemoscope, Niles, IL, USA) instruments in tandem, a set-up permitting the simultaneous analysis of eight samples³⁰. Venous peripheral whole blood was drawn from healthy non-fasting consented donors (three males and eight females, 29–47 years old, with one male and two females studied twice), according to institutional ethics approved protocols. A first blood draw was used to generate chitosan–GP/blood mixtures, and a second blood draw from the same donor was performed within 3 h to analyze unmodified whole blood. Blood was mixed with chitosan–GP at a 3:1 v/v ratio by vigorous shaking for 10 s in glass mixing vials containing six sterile surgical stainless steel mixing beads (0.39 g each, Salem Specialty Ball Co., Canton, CT) as described¹⁷. Unmodified whole blood was transferred to sterile borosilicate mixing vials to control for exposure to glass prior to transferring into TEG reaction cups. TEG plastic reaction cups (made of Cyrolite G20) were pre-loaded with 40 µL of either tPA (2 µg/mL in PBS with 4% w/v BSA), or clotting factor diluted in RLS to give the following target concentrations after adding 320 µL sample: 0.08–10 U/mL IIa; 5 µg/mL rhFVIIa; 0.7–278 pM TF; and rhFVIIa + TF (5 µg/mL rhFVIIa + 0.7 pM TF). Clot tensile strength was recorded manually as the amplitude (the distance in mm on the y-axis between the two traces). At set time intervals, the whole reaction cup was transferred to ice cold quench buffer (20 mM 4-(2-hydroxyethyl)-1-piperazineethanesulfonic acid (HEPES), 150 mM NaCl, 50 mM ethylenediaminetetraacetic acid (EDTA), 10 mM benzamidine, 33 µM FPR-ck, pH 7.4) at a 1:9 ratio of blood:quench buffer, vortexed for 10 s, cleared by a double centrifugation (2500g, 15 min, 4°C) and kept as aliquots at –80°C until analyzed for thrombin generation by TAT ELISA³⁰, or by Western blot for platelet activation by appearance of serum PF4³¹ and for activation of FXIII as determined by cleavage of FXIII A subunit³². The equivalent of 4 µL serum, also adjusted for dilution of blood by chitosan–GP, was loaded into each well of a 17.5% acrylamide non-reducing sodium dodecyl sulfate polyacrylamide gel electrophoresis (SDS-PAGE) for PF4 and 2 µL serum on a 10% acrylamide SDS-PAGE reducing gel for the A and B subunits of FXIII. Proteins were transferred to polyvinylidene fluoride (PVDF) membrane, blocked for 1 h with 5% non-fat milk powder in 50 mM Tris, 150 mM NaCl, 0.1% Tween-20 pH 7.4 (TBST) at 50°C, and probed with goat anti-PF4 (0.2 µg/mL) then 1:10,000 diluted affinity-purified donkey anti-goat-HRP (0.08 µg/mL) or Sheep anti-human A and B subunits of FXIII antibody (9.8 µg/mL) and donkey anti-sheep-HRP (0.08 µg/mL), followed by chemiluminescence (Lumi-Light). Purified proteins were used as positive controls for PF4 (20 ng/well) and FXIII (0.22 µg/well).

IN VIVO ARTICULAR CARTILAGE REPAIR MODEL

All animal experimentation was carried out with protocols approved by the University of Montreal Animal Division, using skeletally mature New Zealand White rabbits ($N = 33$ rabbits, 16 males, 17 females, >8 months randomly assigned to different groups; 8 out of these 33 rabbits received bilateral knee implants for a total of $N = 41$ unilateral or bilateral defects treated with implant, see Table I). Rabbits were anesthetized with an intramuscular injection of ketamine–xylazine–buprenorphine cocktail then placed under 3% isoflurane/8% oxygen gas anesthesia. They were subjected to small knee arthrotomies in order to create bilateral 3.5 × 4 mm

Table I
Experimental design: in vivo solidification time without and with clotting factor

Treatment group	Number of defects	Clotting factor	Technique used to apply clotting factor
1	9	None	—
2	4	rhFVIIa*	Pre-mix with blood
3	5	rhFVIIa† + TF‡	Pre-load on defect, ~60 s delay
4	19§	Ila	Pre-load on defect, ~60 s delay
5	4	Ila¶	Pre-load on defect, 10 s delay

*10 µg/mL (200 nM).

†5 µg/mL (100 nM).

‡4.75 nM.

§N = 9, chitosan–GP/blood, N = 10, RITC–chitosan–GP/blood.

|| 15 or 45 U/mL.

¶45 U/mL.

trochlear defects debrided into the calcified layer¹⁷. All defects were pierced with microdrill holes (either two distal 0.9 mm drill holes and six proximal 0.5 mm drill holes, or four 0.9 mm drill holes) with constant irrigation of cold sterile RLS buffer to keep cartilage humid as previously described^{15,17}. Fresh non-activated autologous rabbit blood was drawn from the central ear artery and mixed at a 3:1 v/v ratio with chitosan–GP. For some implants, 500 µL of chitosan–GP was further combined with 100 µL RITC–chitosan prior to mixing with 1.5 mL blood (see Table I, treatment group 4). Control chitosan–GP/blood implants were delivered from a 1 cc syringe and 20 gauge needle as one hanging drop without clotting factor. In some defects, rhFVIIa was mixed into whole blood to obtain 10 µg/mL rhFVIIa (200 nM) prior to combining with chitosan–GP. In other defects, 3 µL of concentrated clotting factor was pipetted on the defect surface ~60 s prior to liquid implant, either Ila (15 or 45 U/mL, for a target final concentration of 2 or 6 U/mL, respectively) or rhFVIIa + TF [5 µg/mL rhFVIIa and 4.75 nM TF] (see Table I). Finally, in four defects, thrombin (45 U/mL) was “co-delivered” by pipetting 3 µL of on the defect surface within 10 s of applying chitosan–GP/blood implant. *In situ* solidification time of the hybrid clot implants was noted for each implant according to

the animal surgeon’s observations. After re-positioning the patella, knees were closed in sutured layers.

STATISTICAL ANALYSIS

Statistica (version 6.1, StatSoft, Tulsa, OK, USA) software was used for multivariate correlation analysis to test TAT as a predictor of clot tensile strength, and the non-parametric Kruskal–Wallis test to evaluate the effect of clotting factor on *in vivo* implant solidification time. The Student *t*-test was used to determine the effect of chitosan–GP on maximum amplitude, of added clotting factors on clotting time and clot tensile strength at 5 and 15 min. *P* < 0.05 was considered to be significant.

Results

BIPHASIC SOLIDIFICATION OF CHITOSAN–GP/BLOOD MIXTURES

Unmodified whole blood coagulated in the plastic TEG sample cup around 15 min after sample deposition [Fig. 1(A)]. By contrast, chitosan–GP/blood solidified in an atypical biphasic manner, with a rapid and stable increase in viscosity that at 5 min was significantly higher than whole blood [*P* < 0.001, 1.1 vs 0.2 mm, Fig. 1(B) and (C)]. The polymer–blood initial amplitude was also ~3× greater than that of the viscous chitosan solution prior to mixing with GP and blood, and 5× greater than chitosan–GP mixed with water instead of blood (Table II). These data demonstrated that the rapid thickening of chitosan–GP/blood mixtures was due to polymer–blood interactions. Chitosan–GP/blood mixtures had an average clotting time of 21 min, and fully solidified over an average 66 min period, while unmodified whole blood took an average 43 min to reach peak clot strength [time to maximum amplitude, TMA, Fig. 1(C)]. The peak clot tensile strength was similar for whole blood and chitosan–GP/blood [55.2 vs 51.8 mm, Fig. 1(C)]. Addition of tPA at 10-fold higher concentration over normal plasma levels^{33,34} completely dissolved whole blood clots after 2 h [Fig. 1(A) and (C)], while

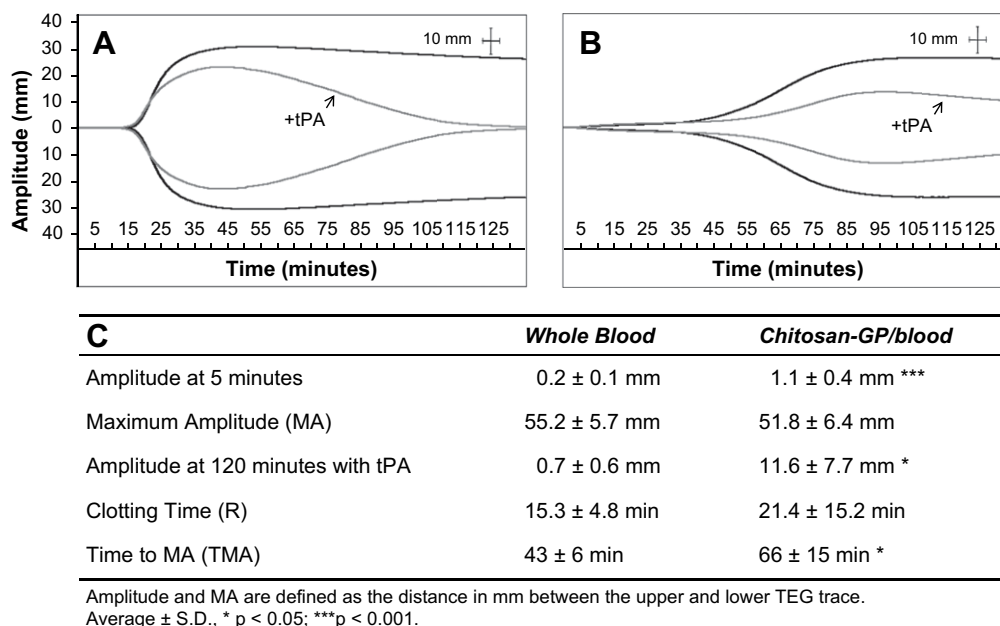


Fig. 1. Clot formation monitored by TEG showed that chitosan–GP/blood has higher initial viscosity, delayed solidification, and similar clot tensile strength compared to whole blood. Representative TEG trace from a non-fasting healthy subject of whole blood (A) and of chitosan–GP/blood mixture (B), without and with tPA (as indicated). (C) Comparative development of clot tensile strength over time in whole blood and chitosan–GP/blood (N = 5–12).

Table II
TEG amplitude of viscosity standards and chitosan solutions

	Viscosity (mPa.s)*	Amplitude (mm)†
<i>Viscosity standard</i>		
N62000	198,700	27.0
Silicone oil	100,000	28.0
N1000	1998	0.4
S60	104	0.2
<i>Chitosan solutions</i>		
2% w/v chitosan–HCl	1849	0.4
Chitosan–GP/water	N/A	0.2

N/A: not available.

*At 25°C.

†At 37°C.

chitosan–GP/blood clots resisted complete lysis by tPA at the same concentration [$P < 0.05$, Fig. 1(B)].

THROMBIN, PLATELETS AND FXIII ARE ACTIVATED DURING CHITOSAN–GP/BLOOD SOLIDIFICATION

Whole blood and chitosan–GP/blood solidification was paralleled by the same sequential order of clotting events, starting with thrombin generation at around 15 min followed by burst platelet activation (PF4) (Fig. 2). Western blot analysis of FXIIIa and B subunits revealed a modest depletion of the A

subunit relative to B, immediately prior to peak clot tensile strength, suggesting that proteolytic activation in the A subunit by thrombin had occurred [Fig. 2(B)]. Chitosan–GP/blood mixtures demonstrated a unique, minor platelet activation starting at 5 min, coinciding with the first phase of increased polymer–blood viscosity [see PF4, Fig. 2(B)]. Activation of platelets at these low levels was most probably not triggered by thrombin generation, since TAT was only detected after a 15 min delay in chitosan–blood mixtures. TAT and PF4 levels were sustained in chitosan–GP/blood mixtures up to 75 min [Fig. 2(B)], while both TAT and PF4 levels declined in parallel in whole blood clot serum after peak clot tensile strength was achieved [Fig. 2(A)]. By multivariate correlation analysis, thrombin generation was a highly significant predictor of clot tensile strength for whole blood [$P < 0.00001$, Fig. 2(C)] and chitosan–GP/blood [$P < 0.00001$, Fig. 2(D)]. These data demonstrated that chitosan–GP/blood mixtures, like whole blood, solidified through a thrombin-dependent mechanism.

CLOTTING FACTORS RAPIDLY INCREASE CHITOSAN–GP/BLOOD CLOT TENSILE STRENGTH

Addition of a variety of clotting factors (thrombin, TF, rhFVIIa, or rhFVIIa + TF) to the *in vitro* TEG sample cup prior to addition of whole unmodified blood and chitosan–GP/blood resulted in a striking decrease in clotting time ($P < 0.05$, except for 0.08 U/mL IIa where $P = 0.3$)

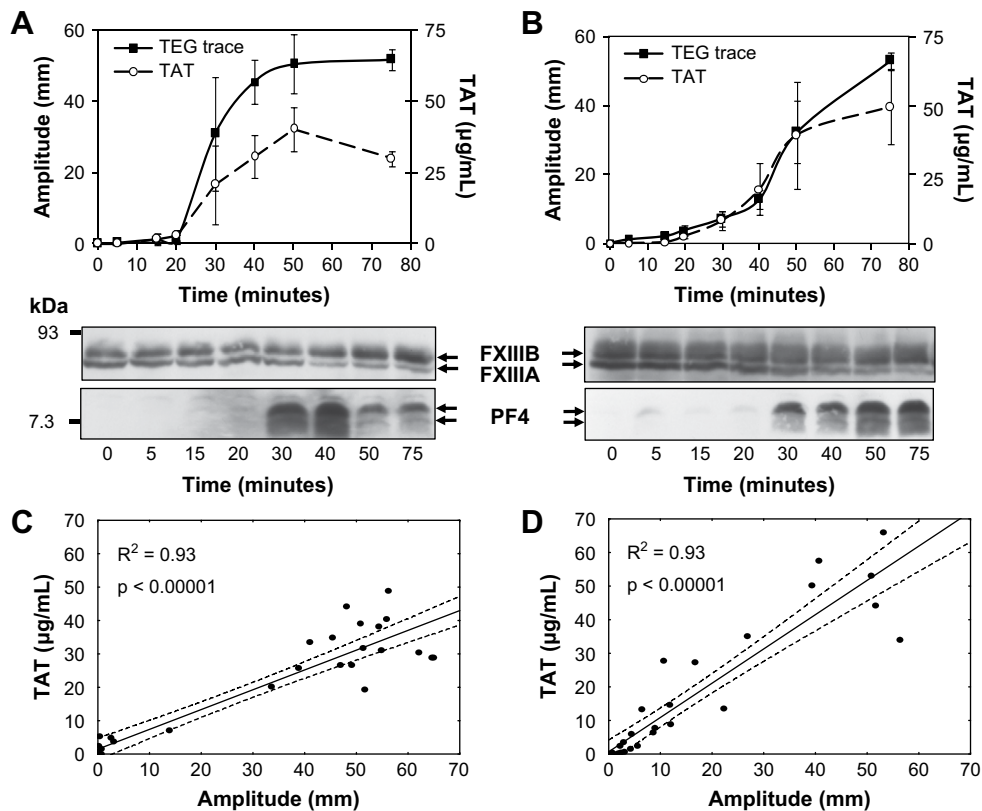


Fig. 2. Solidification of hybrid clots is paralleled by thrombin generation, platelet activation and Factor XIII activation. (A and B) The average amplitude (TEG trace, black line, left y-axis) was superposed with TAT generation (TAT, dashed line, right y-axis) during 75 min for whole blood (A, $N = 3$) and chitosan–GP/blood (B, $N = 4$). Data are given as the mean \pm standard deviation. Western blot analysis of serum samples from TEG experiment showed Factor XIII activation as monitored by proteolytic cleavage and minor diminished intensity of the pro-A subunit relative to the B subunit (middle panels, 50 min+), and platelet activation by the appearance of platelet factor 4 (PF4, bottom panels). (C and D). Linear regression analysis between TAT generation and clot tensile strength (amplitude) over time for whole blood (C, $N = 26$, three donors) and chitosan–GP/blood mixture (D, $N = 32$, 4 donors).

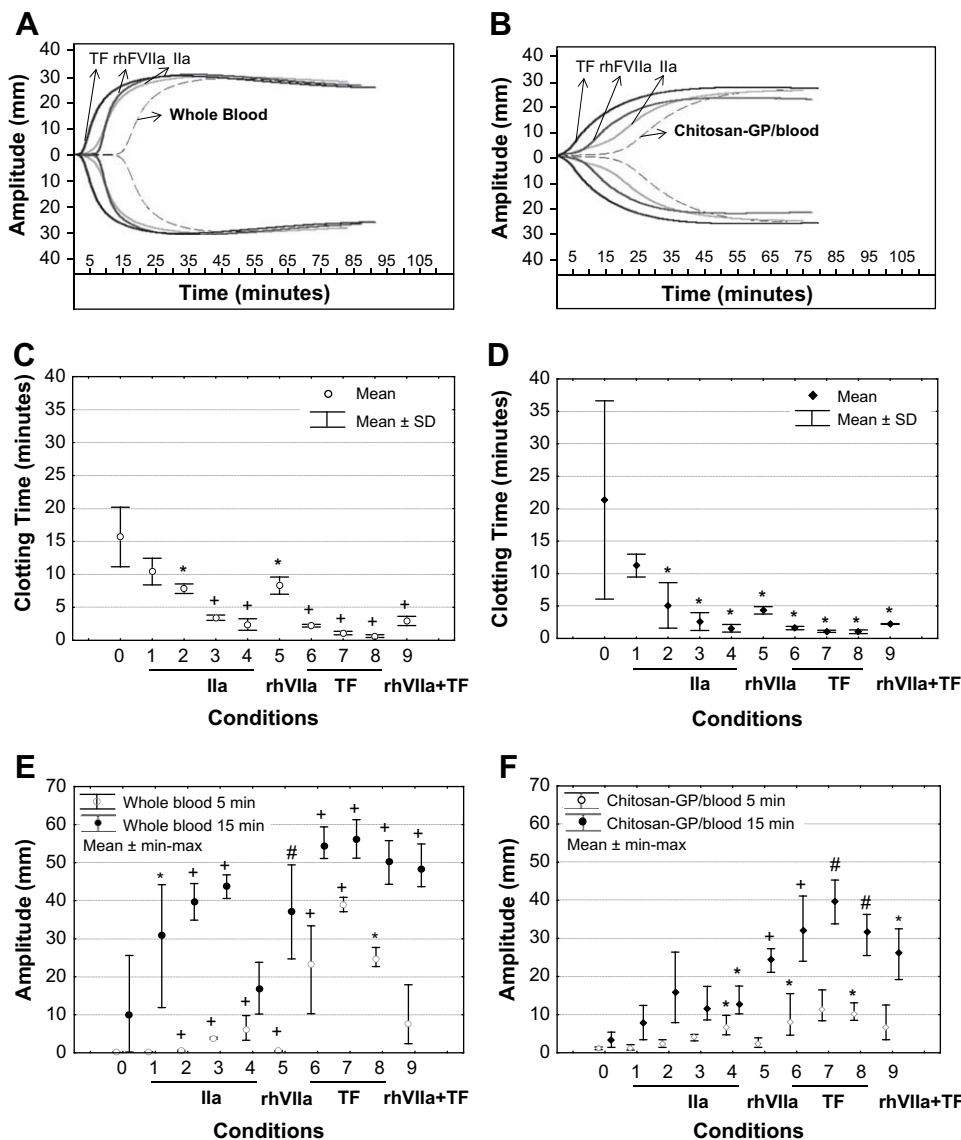


Fig. 3. Clotting factors accelerate *in vitro* solidification of chitosan-GP/blood. Whole blood (A, C, E) and chitosan-GP/blood (B, D, F) were evaluated by TEG with and without clotting factors as indicated. Panels A and B show representative TEG tracings of whole blood (A, dashed line) and chitosan-GP/blood (B, dashed line), and parallel samples with Ila (2 U/mL), rhFVIIa (5 µg/mL), or TF (0.7 pM). The effect of clotting factors on average clotting time (C and D) and average amplitude after 5 and 15 min (E and F) from N = 3 to 6 different human subjects was analyzed for whole blood (C and E) and chitosan-GP/blood (D and F). Conditions: (0) no clotting factor added, (1) 0.08 U/mL Ila, (2) 0.4 U/mL Ila, (3) 2 U/mL Ila, (4) 10 U/mL Ila, (5) 5 µg/mL rhFVIIa, (6) 0.7 pM TF, (7) 7.0 pM TF, (8) 278 pM TF, (9) 5 µg/mL rhFVIIa + 0.7 pM TF. *P < 0.05, #P < 0.01, and +P < 0.005, with respect to sample with no clotting factor.

[Fig. 3(A) and (B)]. The same concentration of clotting factor had a similar ability to shorten the clotting time of unmodified blood and chitosan-GP/blood [Fig. 3(C) and (D)]. However the tensile strength of chitosan-GP/blood mixtures was slower to develop than whole blood [compare 5 vs 15 min., Fig. 3(E) and (F)]. Tissue factor, with or without rhFVIIa, induced the most rapid solidification of chitosan-GP/blood clots [Fig. 3(F)]. Altogether, these data showed that exposure of liquid chitosan-GP/blood mixtures to a small volume of concentrated clotting factor could accelerate solidification *in vitro*. When thrombin was homogeneously mixed into chitosan-GP prior to adding blood, however, the thrombin-polymer-blood mixture rapidly solidified in the mixing vial (unpublished observations). This indicated that clotting factor

should be pre-applied or co-applied to cartilage defects to accelerate *in vivo* solidification.

CLOTTING FACTORS SHORTEN *IN SITU* CHITOSAN-GP/BLOOD IMPLANT SOLIDIFICATION TIME

In microdrilled full-thickness cartilage defects in rabbit trochlea [Fig. 4(A)], chitosan-GP/blood mixtures solidified *in situ* with a delay of 5.0 min [Fig. 4(C), condition 1]. The implant was confirmed as solidified when it no longer ran off the tilted defect or was no longer liquid when probed with a blunt instrument. The time lapse between defect creation and implant loading was between 5 and 10 min, which could theoretically lead to variability in microdrill hole

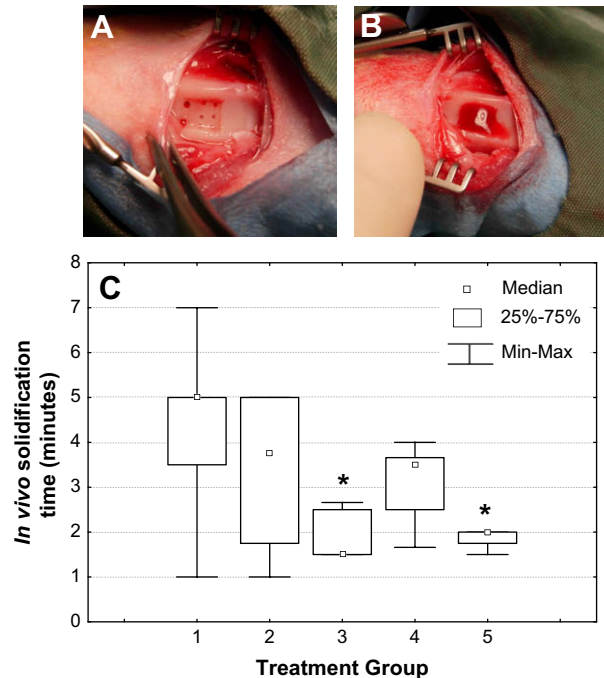


Fig. 4. Effect of added clotting factor and delivery method on *in situ* solidification time of chitosan–GP/blood implant. Trochlear cartilage defect with microdrill holes in rabbit knee before (A) and after (B) chitosan–GP/blood implant deposition with clotting factor. (C) *In situ* solidification time of chitosan–GP/blood with various clotting factor treatments (see Table I for number of defects per treatment group): (1) no clotting factor, (2) rhFVIIa pre-mixed with whole blood, (3) rhFVIIa + TF deposited on defect surface ~60 s prior to implant, (4) IIa deposited on defect surface ~60 s prior to implant, (5) IIa deposited on defect surface 10 s prior to implant. * $P < 0.05$ with respect to implant with no clotting factor.

hemostasis at the time of implant application. However no correlation was found between delay in application and *in situ* solidification time without added clotting factors (data not shown). This suggested that delayed *in situ* solidification was most probably due to a variable delay in clot activation in chitosan–GP/blood mixtures, and in some cases due to a low level of bleeding from subchondral bone.

With the aim of improving the rate of *in situ* solidification, two methods were used to combine clotting factors with chitosan–GP/blood: (1) rhFVIIa was mixed into whole blood prior to combining with chitosan–GP, (2) 3 μ L of clotting factor (thrombin or rhFVIIa + TF) was “painted” on the drilled defect prior to loading a drop of liquid chitosan–GP/blood [Fig. 4(B) and (C), Table I]. Addition of rhFVIIa to chitosan–GP/blood mixtures prior to delivery slightly diminished *in situ* solidification time to 3.75 min, but the effect was not significant [Fig. 4(C), condition 2]. Painting of the defect surface with rhFVIIa + TF ~60 s prior to delivery of chitosan–GP/blood generated the most rapid *in situ*-solidifying implants, 1.5 min [$P = 0.013$, Fig. 4(C), condition 3]. Painting of the defect surface with thrombin ~60 s prior to delivering the implant slightly shortened the average *in situ* solidification time to 3.5 min, but this effect was not significant [Fig. 4(C), condition 4]. By comparison, application of thrombin only 10 s prior to delivering the implant significantly reduced *in situ* solidification time from 5.0 to 2.0 min [$P = 0.021$, Fig. 4(C), condition 5].

Discussion

CHITOSAN–GP/BLOOD CLOTS SOLIDIFY IN A BIPHASIC MANNER INVOLVING POLYMER–BLOOD INTERACTION FOLLOWED BY FIBRIN POLYMERIZATION

Our study has further elucidated the solidification mechanisms of a neutral chitosan–GP/blood mixture, which

generates a cytocompatible implant used for cartilage repair^{17–19}. Chitosan–GP/blood mixtures exhibited an increased initial viscosity by thrombin-independent mechanisms as no significant amount of TAT was detected until 15 min after increased viscosity was observed. Higher viscosity of blood–polymer mixtures could be related to chitosan precipitation or gelation at blood pH which is above the chitosan pK_a ³⁵, to early platelet activation, or to the agglutination of RBCs by chitosan, which has also been previously observed by ourselves and others^{17,21–23}. Chitosan–GP solutions were therefore pro-coagulant in that they generated rapid and low-level platelet activation of the mixture. The latter observation is in agreement with previous reports showing that purified platelets can bind to chitin, to chitosan, and to fibrinogen adsorbed onto chitosan *via* GPIIb/IIIa integrin receptors^{36,37}. Since tPA only partly depressed chitosan–GP/blood clot tensile strength, this demonstrated that both fibrin and chitosan each contributed to the tensile mechanical properties of the hybrid clot. Chitosan–GP/blood clot resistance to tPA provides direct evidence that incorporation of chitosan into whole blood gives rise to a dual fibrin–polysaccharide clot scaffold that is physically more stable than whole blood clots. Therefore hybrid blood clot implants have the potential to sustain the ensuing wound repair response compared to normal whole blood clots.

Platelet activation is known to support the intrinsic clotting cascade^{38,39}, however early and minor platelet activation induced by chitosan–GP was insufficient to accelerate thrombin generation. The more gradual solidification of chitosan–GP/blood relative to whole blood could be related to the 25% dilution of whole blood components, which depresses fibrinogen concentration⁴⁰, to binding of chitosan with fibrinogen⁴¹, to activation of platelets without aggregation in the chitosan–GP/blood mixture, or to slower diffusion

of clotting factors, to their substrate. However it should be noted that the TEG sample cup is made of a non-clot-activating plastic material that does not reflect *in vivo* conditions, where chitosan–GP/blood implant interacts with components present in the débrided cartilage surface such as tissue factor, collagens and extravascular blood from the drilled subchondral bone.

CLOTTING FACTORS DECREASED CLOTTING TIME OF CHITOSAN–GP/BLOOD *IN VITRO* AND *IN VIVO*

All of the clotting factors tested reduced the *in vitro* clotting time of chitosan–GP/blood, and of unmodified whole blood, similar to what is routinely observed using TF to induce *in vitro* coagulation of minimally modified blood and anti-coagulated whole blood^{31,42}. Since TF alone induced the most rapid solidification of chitosan–GP/blood, this suggests that plasma FVII/FVIIa present in the polymer–blood mixtures was capable of rapidly complexing with TF. Rapid coagulation of chitosan–GP/blood in the presence of TF is therefore highly compatible with the natural mechanisms in place to ensure hemostasis of extravascular blood.

Pre-application of rhFVIIa + TF and thrombin *in vivo* to the defect surface reduced the *in situ* solidification time to 1.5 and 2 min, respectively, which represents an important advance towards improving the clinical ease-of-use of chitosan–GP/blood implants. Our data suggest that pre-applied clotting factors induced a more rapid clot activation of the implant, and a more rapid hemostasis of the bleeding drill holes, thus contributing to a faster and more reproducible *in situ* implant solidification time. Even though instant solidification of the implant may be preferred, whole blood coagulation which drives implant solidification is known to require a lag phase during which cellular and enzymatic events need to take place before fibrin polymerization can begin^{25,32}.

We are aware that our evaluation of *in situ* solidification time by the surgeon's observations is somewhat subjective. Even so, our methodology was sufficient to demonstrate that it is important to minimize the delay between delivery of thrombin and implant. Given the naturally high concentration of antithrombin in whole blood³⁹, it is possible that applied thrombin can become gradually inactivated when coming into contact with subchondral blood. Therefore contact between thrombin and the polymer–blood mixture should ideally occur within 10 s, which in the absence of a co-delivery device could be a limiting factor in clinical practice. By comparison, exposure of TF to whole blood is expected to further activate TF, which could explain why TF + rhFVIIa still accelerated implant solidification even after a ~60 s delay in pre-loading. Another limitation of our *in vivo* study was the use of human clotting factors in a rabbit model, although pilot *ex vivo* tests showed that rabbit blood coagulated more rapidly when exposed to all of the human clot factors used (unpublished observations). For clinical applications, human thrombin is preferred over bovine thrombin, given that some patients can develop antithrombin antibodies after even a one-time exposure to bovine thrombin⁴³.

Our study was partly motivated by the knowledge that many clotting factors promote therapeutic effects in wound repair. Tissue factor was previously shown to stimulate angiogenesis⁴⁴ and bone repair in human patients receiving maxillary bone grafts²⁵. Thrombin promotes cell migration and proliferation of many cell types implicated in wound healing of osteochondral defects^{45–47} and stimulates angiogenesis⁴⁸. Chitosan–GP/blood clots demonstrated a longer

TAT generation, and sustained levels of PF4, which could be beneficial to acute repair processes. Platelet factors such as PF4 are known to elicit innate immune cells⁴⁹ and since innate immune activation, angiogenesis, and bone repair have all been identified in the mechanisms of repair by chitosan clot implants^{15,17,19} addition of clotting factors such as purified thrombin, recombinant TF or rhFVIIa have the potential to contribute even further the quality of hyaline repair elicited by these hybrid implants.

Conclusions

Chitosan–GP/blood mixtures solidified through coagulation processes involving thrombin generation, fibrin polymerization and platelet activation and achieved a clot tensile strength similar to whole blood clots. Once solidified, hybrid clots maintained partial tensile strength in the presence of tPA. Hybrid clots demonstrate practical advantages over normal blood clots, as chitosan physically stabilized the clot from lysis and in addition stabilized platelet factor 4 and TAT against rapid degradation in serum after clotting. Clotting factors of the extrinsic clotting cascade and thrombin can be used to accelerate *in situ* solidification of injectable chitosan–GP/blood implants in drilled articular cartilage lesions *in vivo*. Clotting factors have the potential to enhance the practical use, the residency, and therapeutic activity of polymer–blood implants.

Conflict of interest

In support of this research, one or more of the authors received grants or outside funding from BioSyntech, Inc. In addition, one or more of the authors received benefits or agreement to provide benefits from a commercial entity (Bio Syntech, Inc). No commercial entity paid or directed any benefits to any research fund, foundation, educational institution, or other nonprofit organization with which the authors are affiliated.

Acknowledgements

This work was supported by Canadian Institutes of Health Research (CIHR, MOP 144440), salary support to CDH by the Fonds de la Recherche en Santé du Québec (FRSQ) and salary support to CM from the Canadian Arthritis Network (CAN) and FRSQ. We thank Angélique Hoeffler and Francine Dérôme for excellent technical support, Anne Weber for laboratory assistance and Prof. Marie-Claude Heuzey for generously supplying rheology standards.

References

1. Mankin HJ, Johnson ME, Lippello L. Biochemical and metabolic abnormalities in articular cartilage from osteoarthritic human hips. III. Distribution and metabolism of amino sugar-containing macromolecules. *J Bone Joint Surg Am* 1981;63:131–9.
2. Knutsen G, Drogset JO, Engebretsen L, Grontvedt T, Isaksen V, Ludvigsen TC, *et al.* A randomized trial comparing autologous chondrocyte implantation with microfracture. Findings at five years. *J Bone Joint Surg Am* 2007;89:2105–12.
3. Mithoefer K, Scopp JM, Mandelbaum BR. Articular cartilage repair in athletes. *Instr Course Lect* 2007;56:457–68.
4. Insall JN. Intra-articular surgery for degenerative arthritis of the knee. A report of the work of the late K.H. Pridie. *J Bone Joint Surg Br* 1967;49:211–28.
5. Mitchell N, Shepard N. The resurfacing of adult rabbit articular cartilage by multiple perforations through the subchondral bone. *J Bone Joint Surg Am* 1976;58:230–3.

6. Steadman JR, Rodkey WG, Singleton SB, Briggs KK. Microfracture technique for full-thickness chondral defects: technique and clinical results. *Operat Tech Orthop* 1997;7:300–4.
7. Convery FR, Akeson WH, Keown GH. The repair of large osteochondral defects. An experimental study in horses. *Clin Orthop Relat Res* 1972; 82:253–62.
8. Frisbie DD, Trotter GW, Powers BE, Rodkey WG, Steadman JR, Howard RD, *et al.* Arthroscopic subchondral bone plate microfracture technique augments healing of large chondral defects in the radial carpal bone and medial femoral condyle of horses. *Vet Surg* 1999;28:242–55.
9. Hurtig MB, Fretz PB, Doige CE, Schnurr DL. Effects of lesion size and location on equine articular cartilage repair. *Can J Vet Res* 1988;52: 137–46.
10. Mithoefer K, Williams 3rd RJ, Warren RF, Potter HG, Spock CR, Jones EC, *et al.* The microfracture technique for the treatment of articular cartilage lesions in the knee. A prospective cohort study. *J Bone Joint Surg Am* 2005;87:1911–20.
11. Nehrer S, Breinan HA, Ramappa A, Hsu HP, Minas T, Shortkroff S, *et al.* Chondrocyte-seeded collagen matrices implanted in a chondral defect in a canine model. *Biomaterials* 1998;19:2313–28.
12. Saris DB, Vanlauwe J, Victor J, Haspl M, Bohnsack M, Fortems Y, *et al.* Characterized chondrocyte implantation results in better structural repair when treating symptomatic cartilage defects of the knee in a randomized controlled trial versus microfracture. *Am J Sports Med* 2008;36:235–46.
13. Steadman JR, Rodkey WG, Rodrigo JJ. Microfracture: surgical technique and rehabilitation to treat chondral defects. *Clin Orthop Relat Res* 2001;S362–9.
14. Breinan HA, Martin SD, Hsu HP, Spector M. Healing of canine articular cartilage defects treated with microfracture, a type-II collagen matrix, or cultured autologous chondrocytes. *J Orthop Res* 2000;18:781–9.
15. Chevrier A, Hoemann CD, Sun J, Buschmann MD. Chitosan—glycerol phosphate/blood implants increase cell recruitment, transient vascularization and subchondral bone remodeling in drilled cartilage defects. *Osteoarthritis Cartilage* 2007;15:316–27.
16. Hoemann CD, Sun J, Legare A, McKee MD, Buschmann MD. Tissue engineering of cartilage using an injectable and adhesive chitosan-based cell-delivery vehicle. *Osteoarthritis Cartilage* 2005;13:318–29.
17. Hoemann CD, Sun J, McKee MD, Chevrier A, Rossomacha E, Rivard GE, *et al.* Chitosan—glycerol phosphate/blood implants elicit hyaline cartilage repair integrated with porous subchondral bone in microdrilled rabbit defects. *Osteoarthritis Cartilage* 2007;15:78–89.
18. Iliescu M, Hoemann CD, Shive MS, Chenite A, Buschmann MD. Ultrastructure of hybrid chitosan—glycerol phosphate blood clots by environmental scanning electron microscopy. *Microsc Res Tech* 2007;71:236–47.
19. Hoemann CD, Hurtig M, Rossomacha E, Sun J, Chevrier A, Shive MS, *et al.* Chitosan—glycerol phosphate/blood implants improve hyaline cartilage repair in ovine microfracture defects. *J Bone Joint Surg Am* 2005;87:2671–86.
20. Shive MS, Hoemann CD, Restrepo A, Hurtig MB, Duval N, Ranger P, *et al.* BST-Cargel: *in situ* chondroinduction for cartilage repair. *Op Tech Orthop* 2006.
21. Klokkevold PR, Fukayama H, Sung EC, Bertolami CN. The effect of chitosan (poly-*N*-acetyl glucosamine) on lingual hemostasis in hep- arinized rabbits. *J Oral Maxillofac Surg* 1999;57:49–52.
22. Okamoto Y, Yano R, Miyatake K, Tomohiro I, Shigemasa Y, Minami S. Effects of chitin and chitosan on blood coagulation. *Carbohydr Polym* 2003;53:337–42.
23. Rao SB, Sharma CP. Use of chitosan as a biomaterial: studies on its safety and hemostatic potential. *J Biomed Mater Res* 1997;34:21–8.
24. Morrissey JH, Macik BG, Neuenschwander PF, Comp PC. Quantitation of activated factor VII levels in plasma using a tissue factor mutant selectively deficient in promoting factor VII activation. *Blood* 1993;81:734–44.
25. Philippart P, Daubie V, Pochet R. Sinus grafting using recombinant human tissue factor, platelet-rich plasma gel, autologous bone, and anorganic bovine bone mineral xenograft: histologic analysis and case reports. *Int J Oral Maxillofac Implants* 2005;20:274–81.
26. Wilbourn B, Harrison P, Mackie IJ, Liesner R, Machin SJ. Activation of platelets in whole blood by recombinant factor VIIa by a thrombin-dependent mechanism. *Br J Haematol* 2003;122:651–61.
27. Grossman JA, Capraro PA, Burneikis V. Minimizing complications in the use of fibrin sealant in aesthetic facial procedures. *Aesthetic Surg J* 2001;1:32–9.
28. Ma O, Lavertu M, Sun J, Nguyen S, Buschmann MD, Winnik FM, *et al.* Precise derivatization of structurally distinct chitosans with rhodamine B isothiocyanate. *Carbohydr Polym* 2008;72:616–24.
29. Parhami-Seren B, Butenas S, Krudysz-Amblo J, Mann KG. Immunologic quantitation of tissue factors. *J Thromb Haemost* 2006;4:1747–55.
30. Rivard GE, Brummel-Ziedins KE, Mann KG, Fan L, Hofer A, Cohen E. Evaluation of the profile of thrombin generation during the process of whole blood clotting as assessed by thrombelastography. *J Thromb Haemost* 2005;3:2039–43.
31. Rand MD, Lock JB, van't Veer C, Gaffney DP, Mann KG. Blood clotting in minimally altered whole blood. *Blood* 1996;88:3432–45.
32. Brummel KE, Butenas S, Mann KG. An integrated study of fibrinogen during blood coagulation. *J Biol Chem* 1999;274:22862–70.
33. Kahn SR, Solymoss S, Flegel KM. Increased tissue plasminogen activator levels in patients with nonvalvular atrial fibrillation. *CMAJ* 1997; 157:685–9.
34. Thogersen AM, Jansson JH, Boman K, Nilsson TK, Weinehall L, Huhtasaari F, *et al.* High plasminogen activator inhibitor and tissue plasminogen activator levels in plasma precede a first acute myocardial infarction in both men and women: evidence for the fibrinolytic system as an independent primary risk factor. *Circulation* 1998;98: 2241–7.
35. Lavertu M, Filion D, Buschmann MD. Heat-induced transfer of protons from chitosan to glycerol phosphate produces chitosan precipitation and gelation. *Biomacromolecules* 2008;9:640–50.
36. Chou TC, Fu E, Wu CJ, Yeh JH. Chitosan enhances platelet adhesion and aggregation. *Biochem Biophys Res Commun* 2003;302:480–3.
37. Thatte HS, Zagarins S, Khuri SF, Fischer TH. Mechanisms of poly-*N*-acetyl glucosamine polymer-mediated hemostasis: platelet interactions. *J Trauma* 2004;57:S13–21.
38. Butenas S, van't Veer C, Mann KG. Evaluation of the initiation phase of blood coagulation using ultrasensitive assays for serine proteases. *J Biol Chem* 1997;272:21527–33.
39. Kalafatis M, Egan JO, van't Veer C, Cawthern KM, Mann KG. The regulation of clotting factors. *Crit Rev Eukaryot Gene Expr* 1997;7: 241–80.
40. Nielsen VG, Cohen BM, Cohen E. Effects of coagulation factor deficiency on plasma coagulation kinetics determined via thrombelastography: critical roles of fibrinogen and factors II, VII, X and XII. *Acta Anaesthesiol Scand* 2005;49:222–31.
41. Benesch J, Tengvall P. Blood protein adsorption onto chitosan. *Biomaterials* 2002;23:2561–8.
42. Brummel KE, Paradis SG, Butenas S, Mann KG. Thrombin functions during tissue factor-induced blood coagulation. *Blood* 2002;100:148–52.
43. Lollar P. Pathogenic antibodies to coagulation factors. Part II. Fibrinogen, prothrombin, thrombin, factor V, factor XI, factor XII, factor XIII, the protein C system and von Willebrand factor. *J Thromb Haemost* 2005;3:1385–91.
44. Koomagi R, Volm M. Tissue-factor expression in human non-small-cell lung carcinoma measured by immunohistochemistry: correlation between tissue factor and angiogenesis. *Int J Cancer* 1998;79: 19–22.
45. Karp JM, Tanaka TS, Zohar R, Sodek J, Shoichet MS, Davies JE, *et al.* Thrombin mediated migration of osteogenic cells. *Bone* 2005;37: 337–48.
46. Kirilak Y, Pavlos NJ, Willers CR, Han R, Feng H, Xu J, *et al.* Fibrin sealant promotes migration and proliferation of human articular chondrocytes: possible involvement of thrombin and protease-activated receptors. *Int J Mol Med* 2006;17:551–8.
47. Ozaki Y, Nishimura M, Sekiya K, Suehiro F, Kanawa M, Nikawa H, *et al.* Comprehensive analysis of chemotactic factors for bone marrow mesenchymal stem cells. *Stem Cells Dev* 2007;16:119–29.
48. Maragoudakis ME, Tsopanoglou NE, Andriopoulou P. Mechanism of thrombin-induced angiogenesis. *Biochem Soc Trans* 2002;30: 173–7.
49. von Hundelshausen P, Petersen F, Brandt E. Platelet-derived chemokines in vascular biology. *Thromb Haemost* 2007;97:704–13.